PARALLEL MANIPULATORS

Optimised assembly mode reconfiguration of the 5-DOF Gantry-Tau using mixed-integer programming

**Matthew Murray · Geir Hovland ·
Torgny Brogårdh**

Abstract This paper presents a systematic approach based on Mixed Integer Linear Programming for finding an optimal singularity-free reconfiguration path of the 5-DOF Gantry-Tau parallel kinematic machine. The results in the paper demonstrate that singularity-free reconfiguration (change of assembly mode) of the machine is possible, which significantly increases the usable workspace. The method has been applied to a full-scale prototype and the singularity-free path has been verified both in simulations and with physical experiments using real-time control of the prototype. The toolpoint positions have been verified by using measurements from a high precision laser tracker.

Keywords Parallel kinematic machine · Singularity avoidance · Assembly mode · Reconfiguration

1 Introduction

In this paper a new approach for automatically reconfiguring the Gantry-Tau 5-Degrees-of-Freedom (DOF)

M. Murray
University of Queensland, Brisbane, Queensland, Australia
e-mail: murray@itee.uq.edu.au

G. Hovland (✉)
University of Agder, Grimstad, Norway
e-mail: geir.hovland@uia.no

T. Brogårdh
ABB Corporate Research, Västerås, Sweden
e-mail: torgny.brogardh@se.abb.com

parallel kinematic machine (PKM) is presented. The reconfiguration is possible to perform without passing any Type-II singularities and the reconfiguration significantly increases the usable workspace of the robot since two assembly modes of the robot can be reached seamlessly. The concept for calculating the reconfiguration movements is based on a discretisation of the 5-DOF workspace and Mixed Integer Linear Programming (MILP) is used to find the optimal reconfiguration path. The optimisation criterion is to keep the sum of the condition numbers of the manipulator statics matrix as small as possible using a limited number of optimisation steps. The paper presents simulations and experimental results on automatic reconfiguration of a full-scale prototype located at the University of Agder in Norway. During the reconfiguration, as well as during normal operation, only axial forces (and no torsional moments or bending) are transmitted in the 6-links of the Gantry-Tau 5-DOF PKM structure.

In Ref. [1] the difference between working modes and assembly modes for PKMs is defined. Working modes are associated with the different solutions of the inverse kinematics of the PKM, while assembly modes are associated with the different solutions of the forward kinematics. Moreover, a change of a working mode is associated with a serial singularity, i.e. a change of joint position has no effect on tool position. A change of assembly mode is (often) associated with parallel singularities, i.e. the tool cannot resist any effort (gains one or more DOFs) and in turn, becomes uncontrollable. This paper demonstrates that

a change of assembly mode does not necessarily mean that a parallel singularity needs to be passed. An optimisation approach for the 5-DOF Gantry-Tau which changes both assembly and working modes while avoiding parallel singularities is presented. Serial singularities are not avoided, since they can be driven straight through and represent no danger for physical damage of the machine.

In Ref. [2] an approach for reconfiguring the Triglide robot was presented. This approach drives the three linear actuators of the robot from one configuration (or assembly mode) to the other and in this way a larger total workspace of the robot can be achieved. However, the approach requires passing an internal parallel singularity where the tool platform acquires an additional degree of freedom. The described approach is based on force control of one of the actuators and using gravity to pull the tool platform through the singularity. This approach has several disadvantages. First, the joints and the links of the Triglide robot must be able to withstand higher torsional moments. Hence, the links and joints will be unnecessarily over-dimensioned. Second, the tool platform may start to rotate at the singularity and there is no guarantee that gravity will pull the platform through. In fact, this platform rotation must actively be avoided, as the Triglide robot can only be reconfigured if all platform rotations are zero. Moreover, if the platform rotation occurs, gravity may cause large internal forces which can damage the machine. The singularity-free approach presented in this paper allows reconfiguration in both directions of gravity since the tool platform remains fully constrained. It should be mentioned, however, that the reconfiguration method of the Triglide robot described in Ref. [2] is very time-effective caused by the high dynamic of the system and the customised, special joints.

In Refs. [3] and [4] results for a 3-RRR planar parallel manipulator were presented. The authors showed that reconfiguration without passing any singularities was possible. A method for finding singularity-free trajectories based on Octree models and path-connectivity analysis was presented. Unfortunately, the 3-RRR manipulator analysed in the paper has a small workspace to installation space ratio and only 3-DOF with 2-DOF for positioning which limits its use as a general purpose manipulator.

In Ref. [5] the authors presented an analysis based on cusp points to help determine if singularity-free re-

configuration is possible. Cusp points are special coordinates on singularity curves where triple direct kinematic solutions meet in the joint-space for parallel manipulators. It is proven that change of assembly mode is possible through cusp points. The authors presented a systematic approach for finding the cusp points and the method was exemplified for a 3-RPR manipulator.

The results in this paper are interesting for the following reasons: a singularity-free reconfiguration path has been found for a PKM with 5-DOF and a very large workspace to installation space ratio. The authors believe that the 5-DOF Gantry-Tau is one of the most promising PKM structures to date for industrial applications. The Gantry-Tau PKM could even have a higher industrial impact than the successful Delta robot concept described in Ref. [6].

2 The Gantry-Tau structure

The inverse kinematics (IK) of the Gantry-Tau has two solutions for each of the three base actuators for a fixed tool-centre-point (TCP) position and orientation. Hence, there are in total eight possible solutions for the IK. In addition, as illustrated in Fig. 2, the forward kinematics has two solutions for each set of actuator positions. Each of these solutions is typically called assembly mode in the literature, as in the past the only way to change the mode has been to dismount and re-assemble the PKM or to run the PKM through a parallel singularity as in Ref. [2]. Figure 2 illustrates the two most important assembly modes of the Gantry-Tau, where the arms are mounted either all left or all right with respect to the three base actuators. The two assembly modes in Fig. 2 are important because the robot can only reach both of the workspace extremes in these two modes. The kinematics of both the 3-DOF and 5-DOF versions of the Gantry-Tau have been presented before and will not be repeated in this paper. Interested readers can consult Refs. [7, 8].

The approach taken in this paper for reconfiguration is based on the statics matrix **H** of the manipulator. The derivation of this matrix is given as follows.

$$\mathbf{X} = [X\ Y\ Z]^T \qquad \theta = [\alpha\ \beta\ \gamma]^T$$
$$\mathbf{F} = [F_x\ F_y\ F_z]^T \qquad \mathbf{M} = [M_x\ M_y\ M_z]^T$$
$$\mathbf{L} = [l_1\ l_2\ l_3\ l_4\ l_5\ l_6]^T \qquad \mathbf{F}_a = [F_1\ F_2\ F_3\ F_4\ F_5\ F_6]^T$$
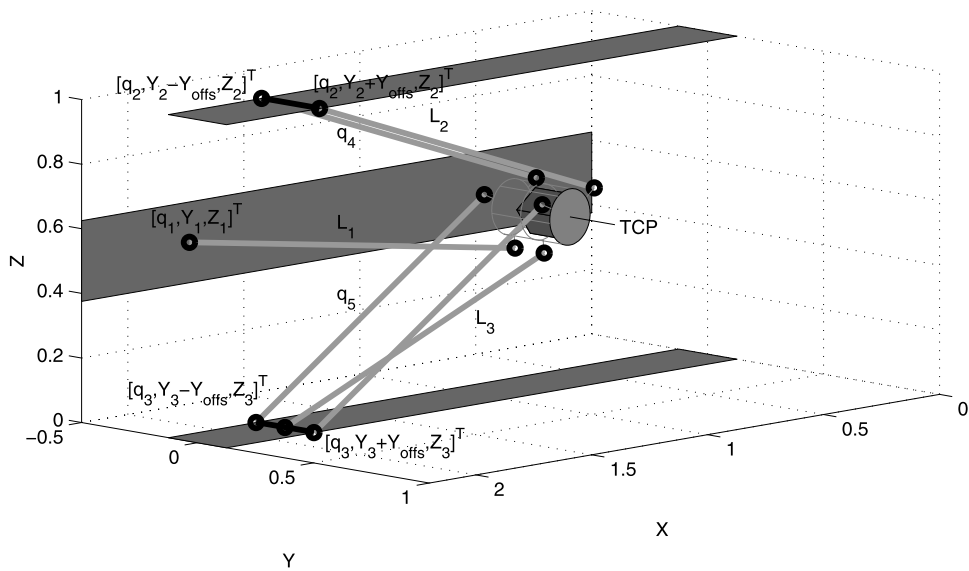
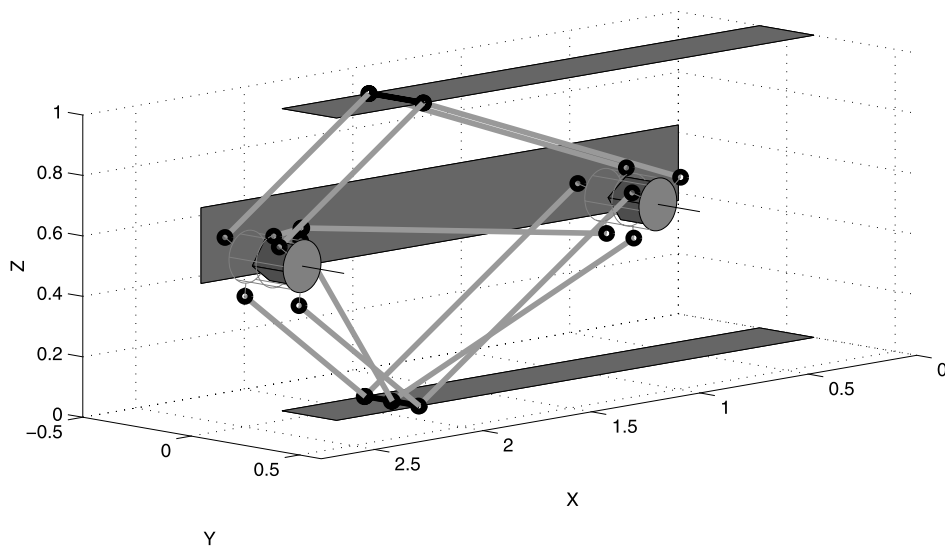**Fig. 1** Triangular link variant of the Gantry-Tau shown in the right-handed configuration for all arms

Fig. 2 The two most important assembly modes for Gantry-Tau, all left and all right

where X, Y, Z are the Cartesian TCP coordinates, α, β, γ are the Cartesian TCP orientation angles, l_i are the link lengths and F_i are link forces where $i = 1, \ldots, 6$. F_x, F_y and F_z are the external Cartesian forces acting on the TCP and M_x, M_y and M_z are the external Cartesian torques acting on the TCP. The relationship between the TCP forces and the link forces are:

$$\mathbf{F} = \sum_{i=1}^{6} F_i \mathbf{u}_i \qquad \mathbf{M} = \sum_{i=1}^{6} F_i \mathbf{A}_i \times \mathbf{u}_i \qquad (1)$$

where $\boldsymbol{u}_i$ is a unit vector in the direction of link i and A_i is a vector pointing from the TCP to the end-point

of link i on the platform. The two equations above can be rewritten using the 6×6 statics matrix $\boldsymbol{H}$.

$$\begin{bmatrix} \mathbf{F} \\ \mathbf{M} \end{bmatrix} = \mathbf{H}\mathbf{F}_a \tag{2}$$

3 Reconfiguration using 5-DOF kinematics

In this section an approach based on Mixed Integer Linear Programming (MILP) optimisation is used to determine an optimal path for automatically reconfiguring the Gantry-Tau PKM while avoiding Type-II singularities.

Figure 3 shows the workspace in the YZ-plane of the Gantry-Tau. This workspace is discretised into smaller spherical regions and each region is associated with a boolean variable named $\delta_{i,j}$. Figure 4 shows the entire state vector $\mathbf{x}$ for the optimisation problem where the optimised path is discretised into N steps. In addition to the region variables $\delta_{i,j}$, the state vector $\mathbf{x}$ contains the following variables for each step i: κ_i (condition number of the PKM statics matrix $\mathbf{H}$ (see (2))), γ_i (boolean help variable to stop optimisation when the goal region j_N has been reached), $P_{i,x}$, $P_{i,y}$, $P_{i,z}$, $R_{i,x}$, $R_{i,z}$ (5-DOF TCP position and orientation) and $a_{i,j}$, $c_{i,j}$ (boolean working mode and working change mode variables for the main actuators $j = 1, 2, 3$).

The optimisation program is given by the following objective function and linear constraints.
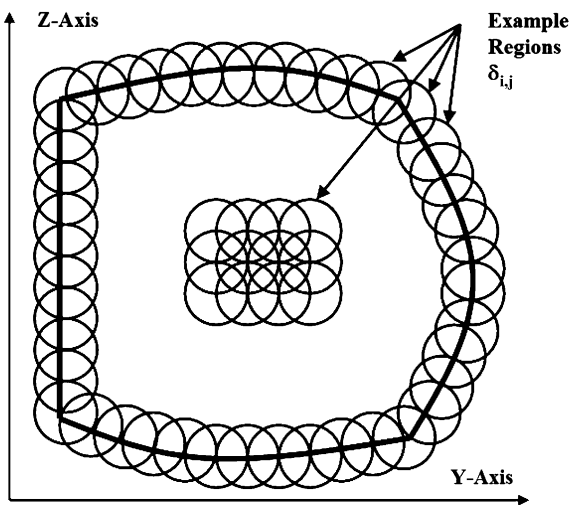
$$\min \ \mathbf{g}^T \mathbf{x} \tag{3}$$

Fig. 3 Example of spherical regions $\delta_{i,j}$

subject to $\mathbf{A}\mathbf{x} \le \mathbf{b}$ \hfill (4)

where $\mathbf{g}$ is the object function vector in (6)–(7) and $\mathbf{A}$, $\mathbf{b}$ given by the constraints in (8)–(38).

Some of the variables in the vector $\mathbf{x}$ are continuous while others are boolean. Hence, the optimisation problem defined by (3)–(4) is referred to as a MILP, see for example Ref. [9]. The state vector $\mathbf{x}$ is formulated as illustrated in Fig. 4. The variables $\delta_{i,j}$ exemplified in Fig. 3 are boolean region variables, while the Cartesian positions at step i, $P_{x,i}$, $P_{y,i}$, $P_{z,i}$, are examples of continuous variables.

The optimisation problem is defined in this case as a minimisation of the sum of the condition numbers of the PKM matrix $\mathbf{H}$ during the reconfiguration path, i.e.

$$\min\left(\sum_{i=1}^{N} \kappa_i \right) \tag{5}$$

Hence, the objective function vector $\mathbf{g}$ equals

$g(k) = 1$ if

$$k \in \left\{ 1, 13 + N_d + 1, \ldots, (13 + N_d)(N - 1) + 1 \right\} \tag{6}$$

$$g(k) = 0 \quad \text{otherwise} \tag{7}$$

The dimension of the vector $\mathbf{g}$ equals $(13 + N_d)N \times 1$, where N_d is the total number of regions $\delta_{i,j}$ for one step i and N the number of optimisation steps. The constant 13 is required because there are 13 variables in each row of Fig. 4 before the region booleans $\delta_{i,j}$. With this definition of $\mathbf{g}$, (3) and (6)–(7) equal (5). The indices in (6) equal the first column in Fig. 4.

Let j_0 be the initial region and j_N be the final goal region. Then, the following constraints are required.

$$\delta_{1,j0} = 1 \tag{8}$$

$$\delta_{1,j} = 0 \quad j \ne j_0 \tag{9}$$

$$\delta_{N,jN} = 1 \tag{10}$$

$$\delta_{N,j} = 0 \quad j \ne j_N \tag{11}$$

where N is the final step number. For each step number i only one state $\delta_{i,j}$ can be set to 1, i.e.

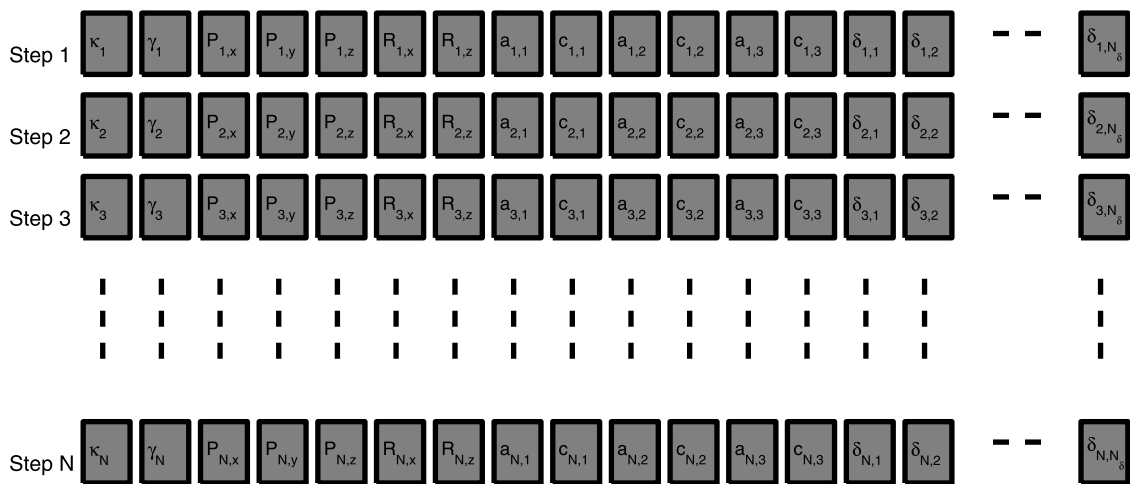$$\sum_{j=1}^{N_\delta} \delta_{i,j} = 1 \tag{12}$$

Fig. 4 Illustration of state vector **x**

In order to prevent that the Cartesian distance between two step numbers becomes too large, a new type of constraint based on the TCP coordinates is introduced as follows.

$$-\Delta X \leq P_{x,i} - P_{x,i-1} \leq \Delta X \tag{13}$$

$$-\Delta Y \leq P_{y,i} - P_{y,i-1} \leq \Delta Y \tag{14}$$

$$-\Delta Z \leq P_{z,i} - P_{z,i-1} \leq \Delta Z \tag{15}$$

$$-\Delta R_x \leq R_{x,i} - R_{x,i-1} \leq \Delta R_x \tag{16}$$

$$-\Delta R_z \leq R_{z,i} - R_{z,i-1} \leq \Delta R_z \tag{17}$$

The constraints in (13)–(17) prevent that the TCP position changes more than the threshold distances ΔX, ΔY, ΔZ between two step numbers. The threshold distances are chosen such that the maximum travelled distance equals the diameter of the region spheres illustrated in Fig. 3. ΔR_x and ΔR_z are the maximum TCP orientation change values, for examples 5 degrees, between two steps.

To set the TCP positions and orientations for each step number i, the following mixed-integer types of constraints are required.

IF $\delta_{i,j} == 1$ THEN $P_{x,i} = X(j)$ (18)

IF $\delta_{i,j} == 1$ THEN $P_{y,i} = Y(j)$ (19)

IF $\delta_{i,j} == 1$ THEN $P_{z,i} = Z(j)$ (20)

IF $\delta_{i,j} == 1$ THEN $R_{x,i} = R_x(j)$ (21)

IF $\delta_{i,j} == 1$ THEN $R_{z,i} = R_z(j)$ (22)

For example, the logical constraint in (18) can be implemented by two linear constraints as follows.

$$-m\delta_{i,j} + P_{x,i} \leq X(j) - m \tag{23}$$

$$M\delta_{i,j} - P_{x,i} \leq -X(j) + M \tag{24}$$

where m, M are the minimum and maximum values of $X(j)$ respectively, see for example Ref. [10] for examples of such logical constraints.

The following logical constraints ensure that the summation of the condition numbers in (5) stops once the final goal region j_N has been reached.

IF $\delta_{i,j} == 1$ THEN $\kappa_i = \gamma_i \kappa(j)$ (25)

IF $\delta_{i,jN} == 1$ THEN $\gamma_i = 0$

ELSE $\gamma_i = 1$ (26)

The IF-THEN-ELSE type of logical constraint in (26) can be implemented by the following four linear constraints.

$$0.99\delta_{i,jN} + \gamma_i \leq 1 \tag{27}$$

$$-1.01\delta_{i,jN} - \gamma_i \leq -1 \tag{28}$$

$$1.01\delta_{i,jN} + \gamma_i \leq 1.01 \tag{29}$$

$$-0.99\delta_{i,jN} - \gamma_i \leq -0.99 \tag{30}$$

The constants 0.99 and 1.01 are chosen as the lower and upper limit of the value 1 in (26). The general logical rules for an IF-THEN-ELSE statement are shown in (31)–(35), where m_1, m_2 and M_1, M_2 are the lower

Fig. 5 The reconfiguration sequence of 25 positions on the 5-DOF Gantry-Tau at the University of Agder as optimised by CPLEX (sequence moves from *left* to *right* and *top* to *bottom*)
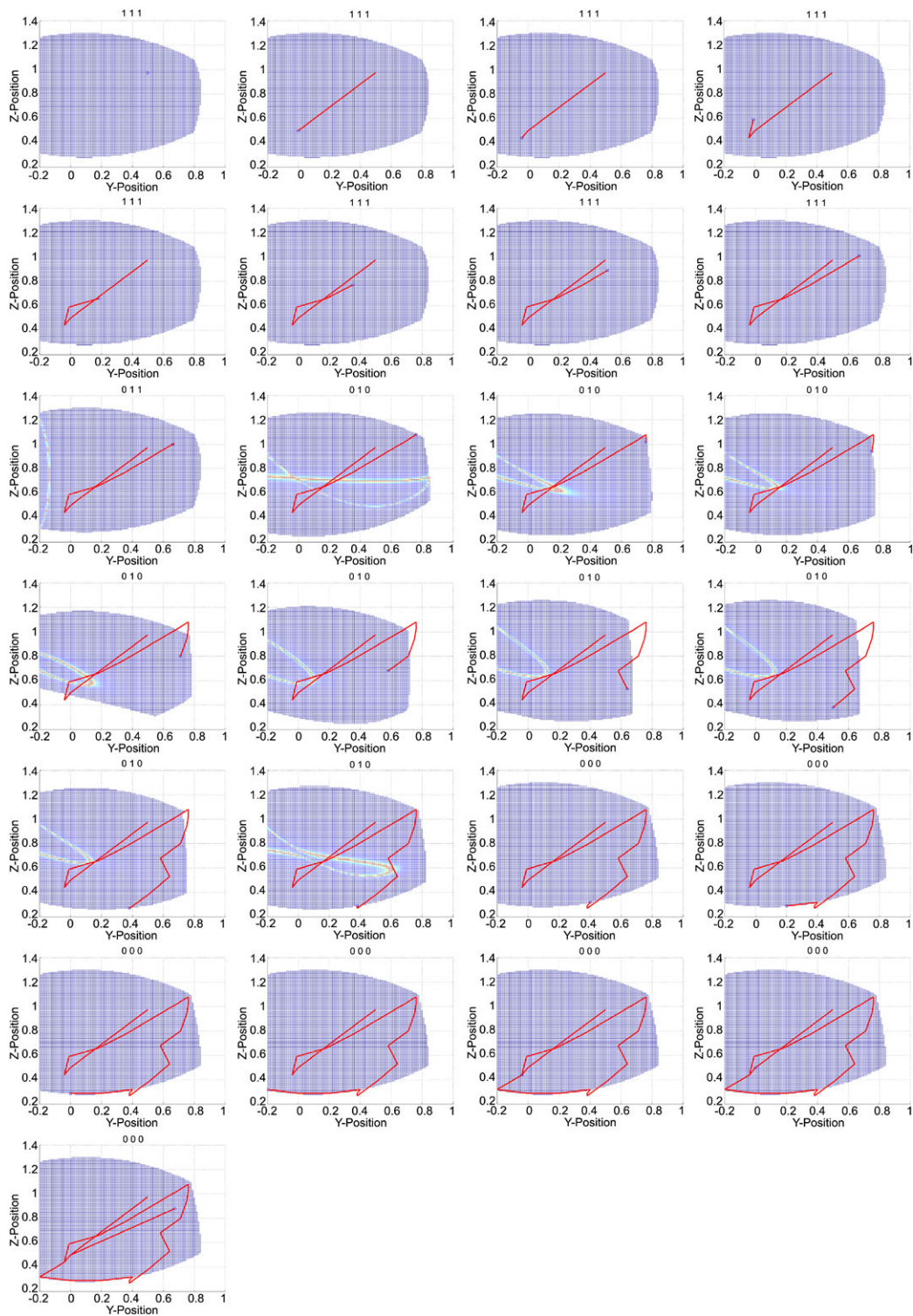
Fig. 6 Optimised path of TCP (*thick solid line*) in the YZ-plane with corresponding condition number maps (*light blue loops*). The sequence moves from *left* to *right* and *top* to *bottom* and corresponds to Fig. 5. Singularities are present in the workspace step 8 to 17
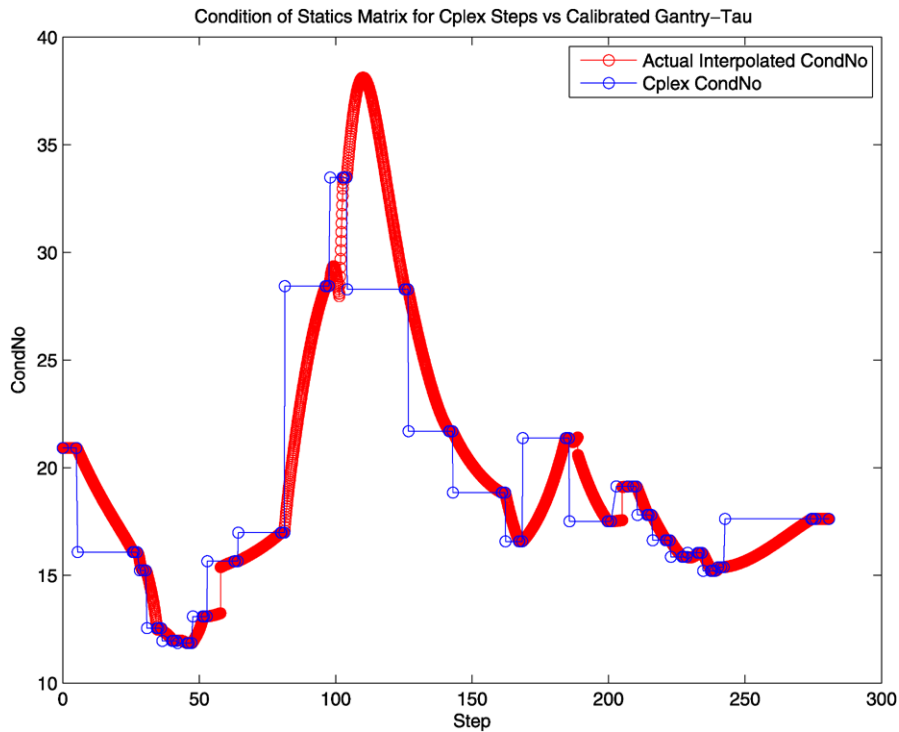
Fig. 7 Condition number of matrix H along the optimised reconfiguration path illustrated in Figs. 5 and 6

and upper limits on the functions f_1 and f_2, respectively.

$$\text{IF } \delta == 1 \quad \text{THEN } z = f_1 \text{ ELSE } z = f_2 \tag{31}$$

$$(m_2 - M_1)\delta + z \leq f_2 \tag{32}$$

$$(m_1 - M_2)\delta - z \leq -f_2 \tag{33}$$

$$(M_2 - m_1)\delta + z \leq f_1 + (M_2 - m_1) \tag{34}$$

$$(M_1 - m_2)\delta - z \leq -f_1 + (M_1 - m_2) \tag{35}$$

$$\text{IF } \delta_{i,j} == 1 \quad \text{THEN } a_{i,k} = A_k(j) \tag{36}$$

$$\text{IF } \delta_{i,j} == 1 \quad \text{THEN } c_{i,k} = C_k(j) \tag{37}$$

$$\text{IF } c_{i-1,k} == 0 \quad \text{THEN } a_{i,k} = a_{i-1,k} \tag{38}$$

The first two logical constraints in (36)–(37) set the current working mode and the working mode change variables equal to the corresponding values for the active region $\delta_{i,j}$. The third logical constraint in (38) sets the current working mode for actuator k ($k = 1, 2, 3$) equal to the working mode for the previous step, if the change variable equals zero. Hence, the working mode for actuator k is only allowed to change at step i if the change variable $c_{i-1,k}$ is equal to 1. In order to formulate the entire MILP optimisation problem, an offline pre-processing step is required which associates the following variables with a region j: $X(j)$, $Y(j)$, $Z(j)$, $R_x(j)$, $R_z(j)$, $\kappa(j)$, $A_k(j)$, $C_k(j)$. $C_k(j) = 1$ represents regions in the workspace for two different working modes where the change of actuator k value approaches zero. $A_k(j) \in [0, 1]$ represents the working mode (left or right) for actuator k for region j.

4 Experiments

Figure 5 shows an example of an optimised reconfiguration path when the actuator lengths are 2.1 m, the support frame has the depth 0.75 m and the height 1.5 m. The arm lengths are 1.09 m for arms 1 and 2, and 1.25 m for arm 3 which correspond to the 5-DOF Gantry-Tau machine located at the University of Agder. Arm 1 consists of the single link, arm 2 consists of a link pair and arm 3 consists of three links including the triangular structure.

Figure 6 shows the optimised path in the YZ-plane of the workspace. A simulation of the actual path of
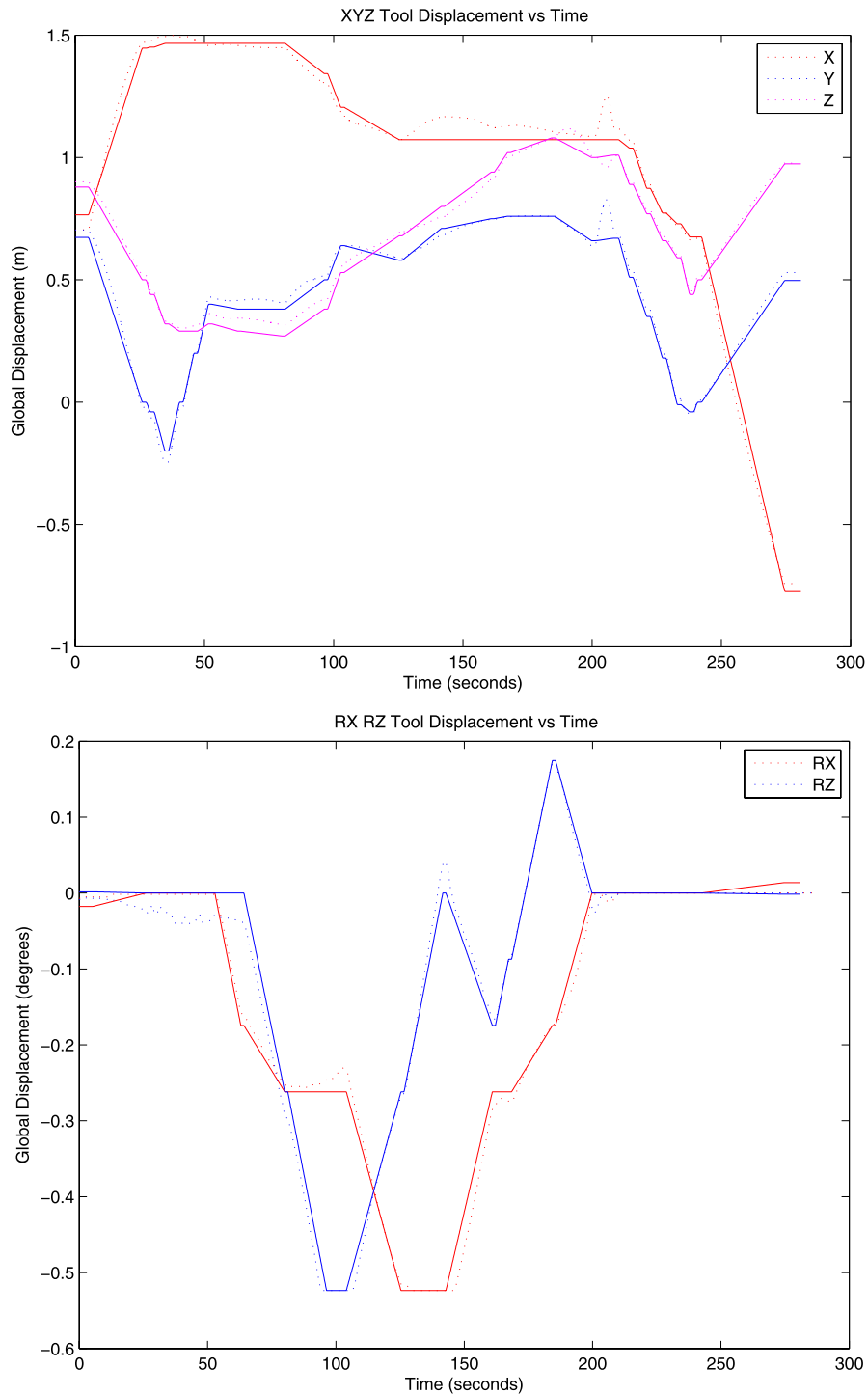
Fig. 8 The path followed during reconfiguration. *Top*: X, Y, Z (*solid*: commanded, *dashed*: measured, *circles*: CPLEX points). *Bottom*: R_x, R_z (*solid*: commanded, *circles*: measured). The maximum tool coordinate system re-orientation is 30 degrees
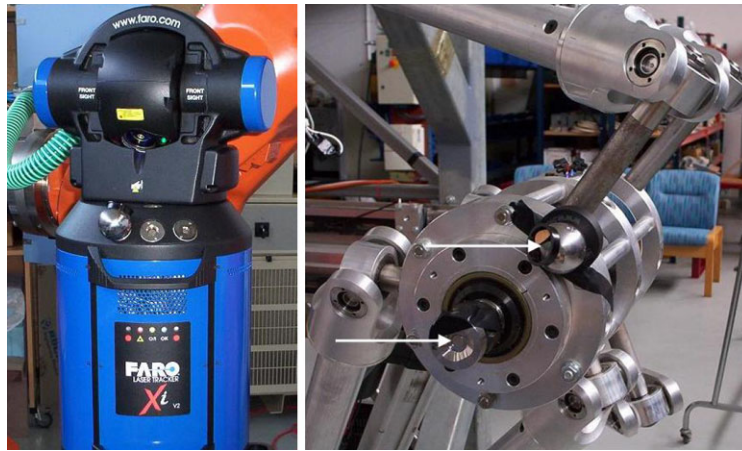
Fig. 9 *Left*: The FARO laser tracker. *Right*: The two reflector locations used to measure the 5-DOF tool path

the TCP is illustrated by the thick solid line, while the actual singularities are marked by the blue lines. For example step 1 has a singularity-free workspace, while step 8 has a large singular loop-shaped area stretching across almost the entire workspace. Note that the X values of the TCP have no influence on the condition number of the statics matrix **H** for the Gantry-Tau.

Figure 7 shows the actual condition number plotted versus the optimisation step number i for the path in Figs. 5 and 6. At Type-II singularities, the condition number of the statics matrix **H** approaches infinity, while Figs. 6 and 7 show that the path is well clear of singular points and the maximum condition number is below 40. The maximum condition number value takes place in the 11th picture in Figs. 5 and 6. The MILP optimisation problem was solved using IBM ILOG CPLEX with a total of $N = 25$ optimisation steps and $N_d = 45936$ region booleans $\delta_{i,j}$ per step. The total number of variables for CPLEX to solve equals $(13 + N_d) * N = 1,148,725$ and the solution time was about 15 minutes on a standard computer. The final interpolated path consisted of 2800 positions with a time step of 10 ms.

In the experimental PKM control shown in Fig. 8 the commanded and measured TCP X, Y, Z, R_x and R_z positions of the optimised reconfiguration path are shown. The tracker can only measure X, Y and Z coordinates. In order to measure the full 5-DOF, the same path was measured twice with two different reflector locations at the tool platform, as illustrated in Fig. 9. In order to accurately estimate both tool angles R_x and R_z, any two reflector locations on the tool platform

can be used. The only requirement is that the vector between the two reflector locations must not coincide with either the TCP x or z axis. Alternatively, a third reflector location and measurement set could be used. Note that the tool angles estimated in Fig. 8 match well with the commanded angles.

The tool rotations of the 5-DOF Gantry-Tau are defined in the following order: First a rotation about the dependent angle R_y, followed by R_z and then R_x. In order to solve for R_x and R_z from measurements of a single vector as given by the two reflector locations shown in Fig. 9, the dependent angle R_y must be known. The angle R_y is calculated as described by the 5-DOF inverse kinematics presented in Ref. [7] from the commanded TCP positions X, Y, Z and the commanded angles R_x and R_z.

The accuracy of the measured TCP X, Y, Z positions match the commanded positions well for 3-DOF motion. For 5-DOF motion the errors are larger, caused mainly by inaccuracies in the kinematic model parameters but also the dynamics of the telescope actuators. The experiments demonstrate, however, that the kinematics do not have to be 100% accurately calibrated for the singularity-free reconfiguration approach presented in this paper to work.

5 Conclusions

This paper has demonstrated that Type-II singularity-free reconfiguration of the 5-DOF Gantry-Tau parallel kinematic machine is possible. The experiments

demonstrated in Fig. 5 were conducted without experiencing any unwanted rotations of the manipulated platform, also when moving the tool platform in the opposite direction of gravity. The reconfiguration sequence is optimised and automated and the machine can follow pre-programmed paths to reconfigure in both directions (from left to right and vice versa). Because of the relatively short linear actuators used for the prototype (2.1 m), the possibility to automatically reconfigure the machine nearly doubles the usable workspace. It should be noted that a singularity-free reconfiguration can not be found for the 3-DOF version of the Gantry-Tau. The reconfiguration is only possible by tilting the manipulated platform when approaching Type-II singularities. In the experiments in this paper the tilting angles were limited at 30 degrees.

Future work will consider additional reconfiguration paths than the optimised path presented in this paper, as well as design and analysis of 4-DOF reconfigurable versions of the Gantry-Tau.

References

1. Majou F, Wenger P, Chablat D (2001) The design of parallel kinematic machine tools using kinetostatic performance criteria. In: Proc 3rd intl conf on metal cutting, Metz, France
2. Budde C, Last P, Hesselbach J (2005) Workspace enlargement of a triglide robot by changing working and assembly mode. In: Proc of IASTED intl conf on robotics and applications, Oct 2005, pp 244–248
3. Chablat D, Wenger P (1998) Working modes and aspects in fully parallel manipulators. In: Proc of the 1998 IEEE intl conf on robotics and automation, Leuven, Belgium, pp 1964–1969. doi:10.1109/ROBOT.1998.680601
4. Chablat D, Wenger P (2004) The kinematic analysis of a symmetrical three-degree-of-freedom planar parallel manipulator. In: Symp on robot design, dyn and control, Montreal
5. Zein M, Wenger P, Chablat D (2006) Singular curves and cusp points int the joint space of 3-RPR parallel manipulators. In: Proc of the 2006 IEEE intl conf on robotics and automation, Orlando, Florida, May 2006, pp 777–782. doi:10.1109/ROBOT.2006.1641804
6. Clavel R (1990). Device for the movement and positioning of an element in space. US Patent No 4.976.582, 11 Dec 1990
7. Murray M, Hovland G, Brogårdh T (2006) Collision-free workspace design of the 5-axis Gantry-Tau parallel kinematic machine. In: Proc of the 2006 IEEE/RSJ intl conf on intelligent robots and systems (IROS 2006), Beijing, Oct 2006, pp 2150–2155, doi:10.1109/IROS.2006.282497
8. Hovland G, Choux M, Murray M, Tyapin I, Brogårdh T (2008) The Gantry-Tau—summary of latest development at ABB, university of Agder and university of Queensland. In: 3rd Intl coll robotic systems for handling and assembly, the coll research centre SFB 562, Braunschweig
9. Schrijver A (1986) Theory of linear and integer programming. Wiley, New York
10. Bemporad A, Morari M (1999) Control of systems integrating logic, dynamics and constraints. Automatica 3(35):407–427. doi:10.1016/S0005-1098(98)00178-2